R. & M. No. 3796

R. & M. No. 3796

PROCUREMENT EXECUTIVE, MINISTRY OF DEFENCE

AERONAUTICAL RESEARCH COUNCIL

REPORTS AND MEMORANDA

Stress Analysis of Fibre Reinforced Plates with Polar Orthotropy

By E. H. MANSFIELD

Structures Dept., R.A.E., Farnborough

LONDON: HER MAJESTY'S STATIONERY OFFICE

1977

£4 net

Stress Analysis of Fibre Reinforced Plates with Polar Orthotropy

By E. H. MANSFIELD

Structures Department, R.A.E., Farnborough

Reports and Memoranda No. 3796*
May, 1975

Summary

This Report considers the stress analysis of elastic plates with polar orthotropic properties. The analysis is applicable to fibre reinforced composites in the form of an annulus or curved strip with circumferential fibres. For certain simple loading conditions, including those of pressure, moment and shear, curves are presented which give the maximum stresses for a wide range of composite geometries and elastic properties.

* Replaces R.A.E. Technical Report 75060—A.R.C. 36 239

LIST OF CONTENTS

1. Introduction

It is well known that certain fibres have exceptional longitudinal strength and stiffness properties. When such fibres are embedded in a matrix to form a 'fibre reinforced composite' they can be used in a structural context. The present and increasing use of such composites is paralleled by research aimed at solving the associated structural problems. Considerable progress has been made, for example, in determining the stiffness and stability characteristics of rectangular composite plates[1,2], and in determining the optimum layout of fibres to resist specified loads[3,4].

The present paper focusses attention on composites with curved fibres. Specifically, the analysis relates to an elastic plate with polar orthotropy such that under conditions of plane stress or plane strain there are constant, but generally differing, values of the Young's moduli in the radial and circumferential directions E_r and E_θ, a constant value of the shear modulus $G_{r\theta}$ and constant values of the Poisson's ratios $\nu_{r\theta}$ and $\nu_{\theta r}$. In practice this means that the analysis is applicable to fibre reinforced composites in the form of an annulus or curved strip with circumferential fibres whose density, or fibre volume fraction, is constant. There may also be radial fibres but the requirement of constant density means that such fibres should, strictly speaking, be of varying lengths to accommodate increasing numbers with increasing radial distance. Alternatively, the circumferential fibres may be bonded to an isotropic plate which, itself, may be composed of fibre reinforced laminates in a pseudo-isotropic array (*e.g.* 0 degrees, ±60 degrees). The analysis does not cater for bending of the plate, so that where such bonding occurs the arrangement should be symmetrical about the mid-thickness plane. Also, if there are thickness changes in the plate there will be restrictions arising from the inherent assumptions of plane stress conditions; furthermore, such restrictions will be more stringent[5] than those in the corresponding isotropic case because of the relatively low value of the transverse shear modulus G_{rz}. Finally, in the context of plane strain, the analysis is applicable to a thick-walled circular cylinder with circumferential fibre reinforcement or to a unidirectional fibre reinforced plate formed into a sector of a cylinder, e.g. as shown in Fig. 10. In such applications the modulus E_r, for example, refers to the Young's modulus through the thickness. The multi-laminate case can also be considered provided the number of laminates is sufficiently large to justify the assumption of average values of the moduli through the thickness.

The analysis first considers the simplest stress states, namely those due to internal or external pressure applied to an annular ring or thick-walled circular cylinder. This is followed by the pure bending of a curved strip. The general form of the stress function is next derived and subsequently used for the analysis of the stresses in a curved strip subjected to a shear force, and for a problem of load transfer via a semicircular ring. All but this last problem have, indeed, been formally solved by various elasticians of the Russian school including, in particular, Lekhnitskii whose book[1] contains a comprehensive list of references. The motivation behind the present (independent) treatment was to provide an engineering insight into the behaviour of composites with polar orthotropy. The treatment accordingly differs from earlier work in the extent of the numerical results presented. Furthermore, in the derivation of the general form of the stress function certain differential operators are introduced which markedly simplify the subsequent analysis.

2. Symmetrical Loading of Ring

We consider first the simple case of a ring or annular plate subjected to an arbitrary combination of internal and external pressure as shown in Fig. 1. The ring exhibits polar orthotropic properties, as discussed in the Introduction, so that the stress-strain relations are given by

$$\left.\begin{aligned} \varepsilon_r &= \frac{\sigma_r}{E_r} - \nu_{\theta r}\frac{\sigma_\theta}{E_\theta}, \\ \text{and} \qquad & \\ \varepsilon_\theta &= \frac{\sigma_\theta}{E_\theta} - \nu_{r\theta}\frac{\sigma_r}{E_r}, \end{aligned}\right\} \tag{1}$$

where, from the Reciprocal Theorem.

$$\frac{\nu_{\theta r}}{E_\theta} = \frac{\nu_{r\theta}}{E_r}. \tag{2}$$

For more general types of loading we later require the further relation

$$\gamma_{r\theta} = \frac{\tau_{r\theta}}{G_{r\theta}}. \tag{3}$$

Now if $\tau_{r\theta}$ is zero and σ_r, σ_θ are independent of θ, as in the present problem, the equation of (radial) equilibrium is

$$\sigma_\theta - \frac{d}{dr}(r\sigma_r) = 0, \tag{4}$$

which can be satisfied by the introduction of a stress function Ψ such that

$$\left.\begin{aligned} \sigma_r &= \frac{\Psi}{r}, \\ \text{and} \qquad & \\ \sigma_\theta &= \frac{d\Psi}{dr}. \end{aligned}\right\} \tag{5}$$

By the same token, if the tangential displacement v is zero, as in the present problem, the direct strains can be expressed simply in terms of the radial displacement u:

$$\left.\begin{aligned} \varepsilon_r &= \frac{du}{dr}, \\ \text{and} \qquad & \\ \varepsilon_\theta &= \frac{u}{r}. \end{aligned}\right\} \tag{6}$$

The equation of compatibility is therefore given by

$$\varepsilon_r = \frac{d}{dr}(r\varepsilon_\theta), \tag{7}$$

which can be expressed in terms of Ψ in virtue of equations (1), (2), (5):

$$\left.\begin{aligned} \alpha^2\Psi - r\frac{d\Psi}{dr} - r^2\frac{d^2\Psi}{dr^2} &= 0, \\ \text{where} \qquad & \\ \alpha^2 &= E_\theta/E_r. \end{aligned}\right\} \tag{8}$$

It may be confirmed that equation (8) is satisfied by terms proportional to $r^{\pm\alpha}$, and it follows that the stresses can be expressed in the form

$$\left.\begin{aligned} \sigma_r &= \frac{A}{\rho^{\alpha+1}} + B\rho^{\alpha-1}, \\ \text{and} \qquad & \\ \sigma_\theta &= -\frac{\alpha A}{\rho^{\alpha+1}} + \alpha B\rho^{\alpha-1}, \end{aligned}\right\} \tag{9}$$

where ρ is a nondimensional measure of the radius given by

$$\rho = r/r_1. \tag{10}$$

2.1. Internal Pressure

For the case of uniform internal pressure p_1, say, the constants A, B are to be chosen to satisfy the conditions

$$\left.\begin{aligned} [\sigma_r]_{\rho=1} &= -p_1, \\ \text{and} \qquad & \\ [\sigma_r]_{\rho=\mu} &= 0, \end{aligned}\right\} \tag{11}$$

where

$$\mu = r_2/r_1. \tag{12}$$

Thus

$$\left.\begin{aligned} A &= -p_1\left(\frac{\mu^{2\alpha}}{\mu^{2\alpha}-1}\right), \\ & \\ B &= \frac{p_1}{\mu^{2\alpha}-1}. \end{aligned}\right\} \tag{13}$$

Of particular interest is the maximum value of the hoop stress which occurs at the inner boundary

$$[\sigma_\theta]_{\rho=1} = \alpha p_1\left(\frac{\mu^{2\alpha}+1}{\mu^{2\alpha}-1}\right). \tag{14}$$

As $\mu \to 1$ the hoop stresses increase very rapidly and in Fig. 2 it has been found convenient to express $[\sigma_\theta]_{\rho=1}$ as a multiple of the *nominal* hoop stress $(r_1p_1/(r_2-r_1))$, i.e. the average hoop stress required to equilibrate the internal pressure. This stress ratio can therefore be regarded as a stress concentration factor and, for the fibre reinforced composite, it will be seen that for given values of r_2/r_1 this stress concentration factor can markedly exceed that for an isotropic material.

2.2. External Pressure

The case of uniform external pressure p_2, say, may likewise be considered. In particular the hoop stresses at the inner and outer boundaries are given by

$$\left.\begin{aligned} [\sigma_\theta]_{\rho=1} &= -2\alpha p_2\left(\frac{\mu^{\alpha+1}}{\mu^{2\alpha}-1}\right), \\ \text{and} \qquad & \\ [\sigma_\theta]_{\rho=\mu} &= -\alpha p_2\left(\frac{\mu^{2\alpha}+1}{\mu^{2\alpha}-1}\right). \end{aligned}\right\} \tag{15}$$

In the isotropic case the maximum stress occurs at the inner boundary, but for the fibre reinforced composite it can occur at either boundary depending on the values of E_θ/E_r and r_2/r_1. The maximum stress has been plotted in Fig. 3 as a multiple of the nominal hoop stress $(-r_2p_2/(r_2-r_1))$. When the maximum occurs at the inner boundary the corresponding curve is shown as a broken line: when at the outer boundary as a full line.

For the fibre reinforced composite it will be seen that for given values of r_2/r_1 the maximum hoop stress, which generally occurs at the outer boundary, can be markedly greater than that in an isotropic material.

2.3. Equal Internal and External Pressure

The case of combined internal and external pressures can, of course, be obtained by superposition of the results of Sections 2.1 and 2.2. It is difficult to visualise a practical situation where this might occur but the results for the case of equal internal and external pressure p, say, though largely of academic interest, do highlight the differences between the isotropic and fibre reinforced material. In the isotropic material the hoop and radial stresses are constant throughout and equal to $-p$, but for the fibre reinforced material (with $E_\theta \neq E_r$) this constancy of stresses only occurs for the *cut* ring. For the continuous ring it may be shown that

$$\left.\begin{aligned} [\sigma_\theta]_{\rho=1} &= \alpha p\left(\frac{\mu^{2\alpha}-2\mu^{\alpha+1}+1}{\mu^{2\alpha}-1}\right), \\ \text{and} \qquad [\sigma_\theta]_{\rho=\mu} &= -\alpha p\left(\frac{\mu^{2\alpha}-2\mu^{\alpha-1}+1}{\mu^{2\alpha}-1}\right). \end{aligned}\right\} \tag{16}$$

These results are shown in Fig. 4 which not only indicates high stress concentrations but also shows that the hoop stress at the inner boundary becomes *tensile* for quite modest values of r_2/r_1 and E_θ/E_r. The reason for this change of sign and the high stress concentrations in this and the previous problems is readily understood by a consideration of the limiting case in which $E_r \to 0$. Then the applied pressure is solely resisted by the adjacent circumferential fibres which are necessarily very highly stressed.

3. Pure Bending of Ring

The pure bending of a cut ring or curved strip, as shown in Fig. 1, is also characterised by zero shear stress $\tau_{r\theta}$, and hoop and radial stresses which are independent of θ. But the tangential displacement v is no longer zero and the equation of compatibility must be derived from the general relationships between strain and displacement. Timoshenko[6] shows that these are

$$\left.\begin{aligned} \varepsilon_r &= = \frac{\partial u}{\partial r}, && \text{(a)} \\ \varepsilon_\theta &= \frac{u}{r} + \frac{1}{r}\frac{\partial v}{\partial \theta}, && \text{(b)} \\ \gamma_{r\theta} &= \frac{1}{r}\frac{\partial u}{\partial \theta} + r\frac{\partial}{\partial r}\left(\frac{v}{r}\right) && \text{(c)} \end{aligned}\right\} \tag{17}$$

In the present problem $\gamma_{r\theta}$ is zero and hence, from equation (17(c)),

$$\begin{aligned} \frac{1}{r^2}\frac{\partial^2 u}{\partial \theta^2} &= -\frac{\partial^2}{\partial r \partial \theta}\left(\frac{v}{r}\right) \\ &= \frac{\partial}{\partial r}\left(\frac{u}{r} - \varepsilon_\theta\right), \end{aligned} \tag{18}$$

by virtue of equation (17(b)). The resulting equation from which v has been eliminated may now be combined with equation (17(a)) to eliminate u and thus derive the equation of compatibility:

$$\frac{\partial^2 \varepsilon_r}{\partial \theta^2} - r\frac{\partial \varepsilon_r}{\partial r} + \frac{\partial}{\partial r}\left(r^2\frac{\partial \varepsilon_\theta}{\partial r}\right) = 0. \tag{19}$$

Substitution of equations (1), (2) and (5) into equation (19) enables us to express this in terms of the stress function Ψ:

$$\alpha^2\left(\frac{\Psi}{r}-\frac{d\Psi}{dr}\right)+2r\frac{d^2\Psi}{dr^2}+r^2\frac{d^3\Psi}{dr^3}=0. \tag{20}$$

It may be confirmed that equation (20) is satisfied by terms proportional to $r^{\pm\alpha}$ (as before) and r. Thus the stresses can be expressed in the form

$$\left.\begin{aligned}\sigma_r &= \frac{A}{\rho^{\alpha+1}}+B\rho^{\alpha-1}+C,\\ \text{and}\\ \sigma_\theta &= -\frac{\alpha A}{\rho^{\alpha+1}}+\alpha B\rho^{\alpha-1}+C.\end{aligned}\right\} \tag{21}$$

For the case of pure bending the constants A, B, C must be chosen to satisfy the following conditions,

$$\left.\begin{aligned}&[\sigma_r]_{\rho=1}=[\sigma_r]_{\rho=\mu}=0,\\ \text{and}\\ &\int_{r_1}^{r_2} r\sigma_\theta dr=-M,\end{aligned}\right\} \tag{22}$$

where M is the moment per unit length. Hence we obtain

$$\left.\begin{aligned}\sigma_r &= \frac{M\Gamma}{r_1^2}\left\{\frac{(\mu^{2\alpha}-\mu^{\alpha+1})}{\rho^{\alpha+1}}+(\mu^{\alpha+1}-1)\rho^{\alpha-1}-\mu^{2\alpha}+1\right\},\\ \text{and}\\ \sigma_\theta &= \frac{M\Gamma}{r_1^2}\left\{-\frac{\alpha(\mu^{2\alpha}-\mu^{\alpha+1})}{\rho^{\alpha+1}}+\alpha(\mu^{\alpha+1}-1)\rho^{\alpha-1}-\mu^{2\alpha}+1\right\},\\ \text{where}\\ \Gamma &= \frac{2(\alpha^2-1)}{2\alpha\{(\mu^2+1)(\mu^{2\alpha}+1)-4\mu^{\alpha+1}\}-(\alpha^2+1)(\mu^2-1)(\mu^{2\alpha}-1)}.\end{aligned}\right\} \tag{23}$$

By taking the limit as $\alpha \to 1$ it may be shown that these results agree with those for the isotropic case[6]. The maximum tensile and compressive hoop stresses occur at the inner and outer boundaries, and these are shown in Fig. 5. The stresses are expressed as multiples of $6M/(r_2-r_1)^2$, the nominal maximum stress assuming a *linear* hoop stress distribution. This form of presentation enables the ordinate in Fig. 5 to be interpreted as a stress concentration factor. It will be seen that the fibre reinforced material exhibits greater stress concentrations than the isotropic material but the increases are much smaller than those which occur in a continuous ring under internal or external pressure. What is surprising is the fact that while the maximum hoop stress always occurs at the inner boundary as in the isotropic case, the hoop stress at the outer boundary exceeds the nominal value when E_θ/E_r and r_2/r_1 exceed certain critical values. The reason for this becomes clearer if we look at Fig. 6 which shows the radial distribution of hoop stress in rings in which $r_2/r_1=2$ and $E_\theta/E_r=1$ or 50. (Results for intermediate values of E_θ/E_r are adequately given by linear interpolation.) Compared to the hoop stresses in the isotropic ring those in the fibre reinforced ring exhibit a superimposed S-ing distribution which accentuates the stresses near the inner and outer boundaries at the expense of those towards the mid-thickness.

The radial stress reaches a maximum value at a radius specified by

$$\frac{\partial \sigma_r}{\partial \rho} = 0, \tag{24}$$

whence, from equation (23),

$$\left.\begin{aligned} \rho &= \rho^*, \text{ say} \\ &= \left\{\left(\frac{\alpha+1}{\alpha-1}\right)\left(\frac{\eta^{2\alpha}-\eta^{\alpha+1}}{\eta^{\alpha+1}-1}\right)\right\}^{1/2\alpha}. \end{aligned}\right\} \tag{25}$$

The maximum radial stress σ_r^*, say, given by equations (23) and (25), is shown in Fig. 7 as a multiple of $6M/(r_2-r_1)^2[(\mu^{\frac{1}{2}}-1)/(\mu^{\frac{1}{2}}+1)]$. The introduction of the additional factor $[(\mu^{\frac{1}{2}}-1)/(\mu^{\frac{1}{2}}+1)]$ means that σ_r^* is expressed as a multiple of the nominal maximum assuming a linear hoop stress distribution. [Briefly, if

$$\sigma_\theta = \left(\frac{1+\mu-2\rho}{\mu-1}\right),$$

it follows from equation (4) that

$$\begin{aligned} \sigma_r &= \frac{1}{\rho}\int_1^\rho \sigma_\theta \, d\rho, \\ &= \frac{1}{\mu-1}\left(\mu+1-\rho-\frac{\mu}{\rho}\right), \end{aligned}$$

whose maximum value is $[(\mu^{\frac{1}{2}}-1)/(\mu^{\frac{1}{2}}+1)]$.]

It will be seen that the maximum radial stress is somewhat less in the fibre reinforced case, though the reduction is very small when $r_2/r_1 < 1{\cdot}5$.

3.1. Fibre Failure versus Interlaminar Failure

In a ring under pure moment the maximum value of the radial stress is much smaller than the maximum hoop stress, and in an isotropic material the radial stress has no bearing on failure or the onset of plasticity. However, in a fibre reinforced material with circumferential reinforcement alone the radial stress necessary to cause failure of the matrix or bond is much smaller than the hoop stress necessary to cause failure of the fibres. Thus it is of interest to determine, for example, the critical dividing line between such modes of failure.

The ratio of the maximum hoop stress $[\sigma_\theta]_{\rho=1}$, denoted by σ_θ^*, to the maximum radial stress σ_r^* is shown in Fig. 8 for various values of r_2/r_1 and E_θ/E_r. For unidirectional CFRP, for example, typical values for the ratio of the failing stresses under longitudinal and transverse tension lie in the range 20–30. If we confine attention to values of r_2/r_1 which yield values of $\sigma_\theta^*/\sigma_r^*$ in this range it is seen that the influence of the modulus ratio E_θ/E_r is very small. In particular, if the ratio of failing stresses is 20, say, it follows from Fig. 8 that interlaminar tensile failure will occur before tensile fibre failure if $r_2/r_1 > 1{\cdot}25$, while if the ratio is 30, say, the corresponding range is $r_2/r_1 > 1{\cdot}15$.

3.2. The Flexural Rigidity of the Ring

We conclude our discussion of the pure bending of a cut ring with a determination of the effective flexural rigidity. In this connection it is convenient to express this as a multiple of the flexural rigidity of a straight beam of modulus E_θ, depth (r_2-r_1) and unit width, the length of this straight beam being $\frac{1}{2}(r_1+r_2)\theta$.

The simplest way to determine the effective flexural rigidity is via the displacement v, which is the only displacement component which contributes to a rotation of sections. By the same token it follows from Section 2 that the A and B components of the stresses in equation (21) do not contribute to the rotation and we are left, somewhat surprisingly, with the constant stress component C. The ensuing analysis is accordingly simpler than that for the isotropic case!

If the index c is introduced to identify this constant stress component we can write

$$\sigma_r^c = \sigma_\theta^c = C, \tag{26}$$

and equation (1) shows that the corresponding strain components ε_r^c and ε_θ^c are constants, and hence equations (17) may be readily integrated to yield

$$v = r\theta\left(\varepsilon_\theta^c - \varepsilon_r^c\right) + \text{rigid body terms.} \tag{27}$$

Now the rotation Ω of a section at θ is given by

$$\left.\begin{aligned} \Omega &= -\frac{\partial v}{\partial r}, \\ &= \theta\left(\varepsilon_r^c - \varepsilon_\theta^c\right), \end{aligned}\right\} \tag{28}$$

and hence the change in curvature of the mid-thickness line, whose length is specified by $s = \frac{1}{2}(r_1 + r_2)\theta$, is given by

$$\left.\begin{aligned} \frac{d\Omega}{ds} &= \frac{2(\varepsilon_r^c - \varepsilon_\theta^c)}{r_1 + r_2}, \\ &= \frac{2C(\alpha^2 - 1)}{E_\theta(r_1 + r_2)}, \end{aligned}\right\} \tag{29}$$

in virtue of equations (1) and (26). Also, in terms of an effective flexural rigidity J, say, engineers' theory of bending gives

$$\frac{d\Omega}{ds} = \frac{M}{J}, \tag{30}$$

and hence from equations (23), (29),

$$\left.\begin{aligned} \frac{J}{E_\theta I} &= \frac{6(1+\mu)}{\Gamma(\mu-1)^3(\alpha^2-1)(1-\mu^{2\alpha})} \\ &\\ I &= \frac{1}{12}(r_2 - r_1)^3. \end{aligned}\right\} \tag{31}$$

where

The variation of $J/E_\theta I$ with r_2/r_1 for various values of E_θ/E_r is shown in Fig. 9. It is seen that for the isotropic case the effective flexural rigidity is adequately given by EI for values of r_2/r_1 up to about 3. In contrast, the fibre reinforced case shows a marked reduction in J for all but the smallest values of r_2/r_1.

4. General Loading of Ring

The loadings considered so far have been characterised by the vanishing of one, or both, of the terms $\tau_{r\theta}$ and v, and this has resulted in simplified equations of equilibrium and compatibility. In the general case the equations of equilibrium are[6]

$$\left.\begin{aligned} \frac{\partial \sigma_r}{\partial r} + \frac{1}{r}\frac{\partial \tau_{r\theta}}{\partial \theta} + \frac{\sigma_r - \sigma_\theta}{r} &= 0, \\ &\\ \frac{1}{r}\frac{\partial \sigma_\theta}{\partial \theta} + \frac{\partial \tau_{r\theta}}{\partial r} + \frac{2\tau_{r\theta}}{r} &= 0, \end{aligned}\right\} \tag{32}$$

and

and these are satisfied by the introduction of a stress function Φ such that

$$\left.\begin{aligned}\sigma_r &= \frac{1}{r}\frac{\partial\Phi}{\partial r}+\frac{1}{r^2}\frac{\partial^2\Phi}{\partial\theta^2},\\ \sigma_\theta &= \frac{\partial^2\Phi}{\partial r^2},\\ \tau_{r\theta} &= -\frac{\partial}{\partial r}\left(\frac{1}{r}\frac{\partial\Phi}{\partial\theta}\right).\end{aligned}\right\} \tag{33}$$

As for the equation of compatibility, it may be confirmed by substitution that the general strain displacement relations of equation (17) satisfy the equation

$$\frac{\partial}{\partial r}\left\{r^2\left(\frac{\partial\varepsilon_\theta}{\partial r}-\frac{1}{r}\frac{\partial\gamma_{r\theta}}{\partial\theta}\right)\right\}-r\frac{\partial\varepsilon_r}{\partial r}+\frac{\partial^2\varepsilon_r}{\partial\theta^2}=0. \tag{34}$$

The equation satisfied by the stress function Φ is obtained by substitution of equations (1), (3) and (33) into equation (34). This stress function equation is best expressed in a compact form by introducing the following differential operators defined by:

$$\left.\begin{aligned}\Delta_r F &= r^2\frac{\partial}{\partial r}\left(\frac{F}{r}\right),\\ \text{and}\qquad\\ \Delta_\theta F &= \left(1+\frac{\partial^2}{\partial\theta^2}\right)F.\end{aligned}\right\} \tag{35}$$

It may now be shown that

$$\left.\begin{aligned}&[\kappa\,\Delta_r^4+2\beta\,\Delta_r^2\,\Delta_\theta+\Delta_\theta^2-(1+\kappa+2\beta)\,\Delta_r^2]\Phi=0,\\ &\text{where}\\ &\kappa=E_r/E_\theta\\ &\text{and}\\ &\beta=\frac{E_r}{2G_{r\theta}}-\nu_{r\theta}.\end{aligned}\right\} \tag{36}$$

Note that for the isotropic case

$$\kappa=\beta=1,$$

and the differential operator in equation (36) factorises to give

$$[\Delta_r^2+\Delta_\theta\pm 2\Delta_r]\Phi=0, \tag{37}$$

whence

$$\Phi=\Phi_1+\Phi_2, \text{ say}$$

where

$$\left.\begin{aligned} \nabla^2\Phi_1 &= 0, \\ \Phi_2 - r\frac{\partial\Phi_2}{\partial r} + \frac{1}{4}r^2\nabla^2\Phi_2 &= 0, \end{aligned}\right\} \tag{38}$$

and we recover the biharmonic equation, albeit in a separated and unusual form.

4.1. General Form of the Stress Function

A general expression for Φ can readily be obtained in the form of a series

$$\Phi = \sum_{n=0}^{\infty} \Phi_n, \tag{39}$$

where

$$\Phi_n = \sum_{i=1}^{4} (a_{ni} r^{q_i} \cos n\theta + b_{ni} r^{q_i} \sin n\theta), \tag{40}$$

where the a_{ni} and b_{ni} are constants and the indices q_i are determined below. Substitution of equation (40) into equations (35) and (36) shows that

$$\left.\begin{aligned} \Delta_r\Phi_n &= (q-1)\Phi_n, \\ \Delta_\theta\Phi_n &= (1-n^2)\Phi_n, \end{aligned}\right\} \tag{41}$$

and it follows that for any given value of n there are, in general, four values of q (denoted by q_i) determined by the equation

$$\kappa(q-1)^4 - (q-1)^2(1+\kappa+2\beta n^2) + (n^2-1)^2 = 0. \tag{42}$$

When either q or n equals unity equation (42) results in repeated roots and further analysis is required. Thus if $q = 1$ we must consider the general expression

$$\Phi = rf(\theta). \tag{43}$$

Substitution into equations (35) and (36) shows that

$$\Delta_r\Phi = 0,$$

so that

$$\Delta_\theta^2 f = 0,$$

which may be integrated to give

$$f(\theta) = a_1\theta \sin\theta + b_1\theta\cos\theta + (\text{terms proportional to } \sin\theta \text{ and } \cos\theta, \text{ which do not contribute to the stresses}). \tag{44}$$

By the same token, if $n = 1$ we consider

$$\Phi_1 = g(r)\begin{pmatrix}\sin\\ \cos\end{pmatrix}\theta. \tag{45}$$

Substitution into equation (35) shows that

$$\Delta_\theta \Phi_1 = 0,$$

and hence equation (36) may be expressed in the form

$$g(r) = g_1(r) + g_2(r), \tag{46}$$

where

$$[\kappa \Delta_r^2 - (1 + \kappa + 2\beta)] g_1 = 0, \tag{47}$$

and

$$\Delta_r^2 g_2 = 0. \tag{48}$$

Equation (47) admits of a solution consistent with equation (40), while equation (48) may be integrated to give

$$g_2(r) = cr \ln r + (\text{a term proportional to } r \text{ which does not contribute to the stresses}). \tag{49}$$

Finally, consideration of the limiting case in which $n = 0$ leads us to the solution

$$\Phi_0 = a_{01} + b_{01}\theta + (a_{02} + b_{02}\theta) r^{1+\alpha} + (a_{03} + b_{03}\theta) r^{1-\alpha} + (a_{04} + b_{04}\theta) r^2, \tag{50}$$

where α is as defined in equation (8). In this expression for Φ_0 the term a_{01} does not contribute to the stresses, while the terms identified by a_{02}, a_{03} and a_{04} correspond to the stress function Ψ of Sections 2, 3.

[Note that each of the solutions derived in this section has its counterpart in the general stress function for the isotropic case which was first derived by Michell[7] and is reproduced in Ref. 6. The present analysis, however, shows that two solutions were overlooked in this earlier work, namely

$$\Phi = A\theta \ln r + B\theta r^2 \ln r.]$$

2. Shear Force applied to Curved Strip

The pure bending of a cut ring or curved strip was considered in Section 3. This analysis is augmented here by a consideration of the stresses in a curved strip subjected to shear. A situation in which this would be relevant is shown in Fig. 10 which depicts a section through the edge region of a fibre reinforced plate A where it is attached to another member B at right angles. The edge of the plate has been formed to include an annular quadrant and any transverse loads/pressures acting on the plate may be resolved at section C into a moment M per unit length and a shear force S per unit length. At section D the shear force S is resisted by a moment and a force S which is now parallel to the fibres; the solutions for a moment and shear force can therefore be combined to yield also the solution for a force applied in any direction.

The stresses due to the shear force S may be derived from the stress function of equation (45) which, for convenience, we express in the form

$$\left.\begin{aligned} &\Phi_1 = r_1^2 \sin\theta \left\{ \left(\frac{a_1}{q_1 - 1}\right) \rho^{q_1} + \left(\frac{a_2}{q_2 - 1}\right) \rho^{q_2} + a_3 \rho \ln \rho \right\}, \\ &\text{where} \\ &q_{1,2} = 1 \pm \omega, \\ &\text{and} \\ &\omega = \left(1 + \frac{1 + 2\beta}{\kappa}\right)^{\frac{1}{2}}. \end{aligned}\right\} \tag{51}$$

The derived stresses are given by

$$\left.\begin{aligned}\sigma_r &= \rho^{-2}\sin\theta(a_1\rho^{q_1}+a_2\rho^{q_2}+a_3\rho),\\ \sigma_\theta &= \rho^{-2}\sin\theta(q_1a_1\rho^{q_1}+q_2a_2\rho^{q_2}+a_3\rho),\\ \text{and}\\ \tau_{r\theta} &= -\rho^{-2}\cos\theta(a_1\rho^{q_1}+a_2\rho^{q_2}+a_3\rho),\end{aligned}\right\} \tag{52}$$

and it is to be noted that

$$\sigma_r/\sin\theta = -\tau_{r\theta}/\cos\theta. \tag{53}$$

The boundary conditions along the curved edges are that

$$[\sigma_r = \tau_{r\theta} = 0]_{r=r_1,r_2}, \tag{54}$$

while equilibrium at section C requires that

$$S = -\int_{r_1}^{r_2} \tau_{r\theta}\, dr. \tag{55}$$

Equations (54) and (55) suffice to determine the constants a_i which are given by

$$\left.\begin{aligned}&a_1 = \frac{S}{r_1K}, \qquad a_2 = \frac{S\mu^\omega}{r_1K} \text{ and } a_3 = -\frac{S(\mu^\omega+1)}{r_1K},\\ &\text{where}\\ &K = \frac{2(\mu^\omega-1)}{\omega} - (\mu^\omega+1)\ln\mu.\end{aligned}\right\} \tag{56}$$

It is seen from equation (56) that the elastic properties affect the stresses only insofar as they affect the parameter ω. More directly it is seen that the governing parameter is given by

$$\left.\begin{aligned}\eta, \text{ say} &= \frac{1+2\beta}{3\kappa}\\ &= \frac{1}{3}\left\{E_\theta\left(\frac{1}{E_r}+\frac{1}{G_{r\theta}}\right) - 2\nu_{\theta r}\right\},\end{aligned}\right\} \tag{57}$$

where the factor $1/3$ has been introduced so that $\eta = 1$ in the isotropic case.

The variation of the hoop and shear stresses through the thickness of the curved sheet (or beam) is shown in Figs. 11, 12 for the case in which $r_2/r_1 = 2$ and $\eta = 1$ or 50. If the hoop stresses are compared with those in Fig. 6, which relates to an applied moment, it is seen that for equal values of E_θ/E_r and η the hoop stresses in the fibre reinforced case exhibit a greater degree of *S*-ing due to an applied shear force. This is reflected in Fig. 12 in a flatter distribution of the shear stress.

The maximum value of the hoop stress occurs at $\theta = \frac{1}{2}\pi$, $r = r_1$, and is given by

$$\sigma_{\theta,\max} = \frac{S\omega(1-\mu^\omega)}{r_1K}, \tag{58}$$

which is shown in Fig. 13 where $\sigma_{\theta,\max}$ has been expressed as a multiple of $r_2S/(r_2-r_1)^2$ in order to flatten the curve for the isotropic case and so high-light the influence of anisotropy.

The shear stress and the radial stress reach maximum values at a radius specified by

$$\rho^{**}, \text{ say} = \mu\left(\frac{2(\omega+1)}{(\mu^{\omega}+1)^2+4\mu^{\omega}(\omega^2-1)\}^{\frac{1}{2}}+\mu^{\omega}+1}\right)^{1/\omega}, \tag{59}$$

and Fig. 14 shows the corresponding values of $\tau_{r\theta,\max}$ expressed as a multiple of $-S/(r_2-r_1)$. It is seen that as $r_2/r_1 \to 1$ this stress ratio approaches 1·5 which is the value appropriate to a parabolic distribution of shear. Deviations from this value are comparatively modest. Fig. 14 is, of course, also applicable to $\sigma_{r,\max}$ in virtue of equation (53).

4.3. Load Transfer via Semi-circular Ring

As a further example in the use of the general stress function we consider a purely circumferentially fibre reinforced semi-circular ring with contiguous fibre-reinforced parallel strips as shown in Fig. 15a. A force P per unit length is applied along the line $\theta = 0$, via a pin of radius r_1, and is resisted by loads of magnitude $\frac{1}{2}P$ in each of the strips. Strictly speaking this is a difficult contact problem which requires a knowledge of the clearance and frictional properties between pin and ring, and the elasticity and support conditions of the pin, etc. As such it is outside the scope of the present paper but the essential features may, nevertheless, be reproduced. Thus, to simplify the problems we will assume that along the interface between pin and ring the radial stress varies as $\cos^2\theta$, so that

$$\left.\begin{aligned}[\sigma_r]_{r=r_1} &= -\frac{3P}{8r_1}(1+\cos 2\theta),\\ \text{and}\qquad [\tau_{r\theta}]_{r=r_1} &= 0,\end{aligned}\right\} \tag{60}$$

while across the sections at $\theta = \pm\frac{1}{2}\pi$,

$$\left.\begin{aligned}[v]_{\theta=\pm\frac{1}{2}\pi} &= 0,\\ \text{and}\qquad [\tau_{r\theta}]_{\theta=\pm\frac{1}{2}\pi} &= 0.\end{aligned}\right\} \tag{61}$$

These boundary conditions are the same as those in a complete ring subjected to 'mirror image' loads as shown in Fig. 15b. The solution corresponding to the constant stress component in equation (60) is given in Section 2.1 while the solution for the part which varies as $\cos 2\theta$ can be obtained from the stress function

$$\Phi_2 = r_1^2 \cos 2\theta \sum_{i=1}^{4} a_i \rho^{q_i}, \tag{62}$$

where the indices q_i are the roots of the equation

$$\kappa(q-1)^4-(q-1)^2(1+\kappa+8\beta)+9=0, \tag{63}$$

and, for convenience, we have reintroduced the nondimensional term $\rho(=r/r_1)$.

Substitution of equation (62) into equation (33) gives

$$\left.\begin{aligned}\sigma_r &= \cos 2\theta \sum_i (q_i-4)a_i\rho^{q_i-2},\\ \sigma_\theta &= \cos 2\theta \sum_i q_i(q_i-1)a_i\rho^{q_i-2},\\ \text{and}\qquad \tau_{r\theta} &= \sin 2\theta \sum_i (q_i-1)a_i\rho^{q_i-2}.\end{aligned}\right\} \tag{64}$$

The boundary conditions of equation (61) are automatically satisfied by the expression for Φ_2, while the vanishing of σ_r and $\tau_{r\theta}$ at $r = r_2$ (i.e. $\rho = \mu$) implies that

$$\left.\begin{aligned} &\sum_i a_i \mu^{q_i} = 0, \\ &\text{and} \\ &\sum_i (q_i - 1) a_i \mu^{q_i} = 0. \end{aligned}\right\} \tag{65}$$

Similarly equations (60) can be combined to yield

$$\left.\begin{aligned} &\sum_i a_i = \frac{P}{8r_1}, \\ &\text{and} \\ &\sum_i (q_i - 1) a_i = 0. \end{aligned}\right\} \tag{66}$$

Equations (65) and (66) suffice to determine the coefficients a_i and hence the maximum value of σ_θ, which occurs at the points $r = r_1$, $\theta = \pm\frac{1}{2}\pi$, can be determined from the relation

$$\sigma_\theta^*, \text{ say} = \sum_i q_i (q_i - 1) a_i. \tag{67}$$

As for the constant stress component in equation (60) it will be seen by comparison with equations (11) and (14) that the maximum value of σ_θ is given by

$$\sigma_\theta^{**}, \text{ say} = \frac{3\alpha P}{8r_1}\left(\frac{\mu^{2\alpha} + 1}{\mu^{2\alpha} - 1}\right). \tag{68}$$

Thus, in the problem under consideration the maximum value of σ_θ is given by

$$\sigma_{\theta,\max} = \sigma_\theta^* + \sigma_\theta^{**}. \tag{69}$$

Calculations have been made for the following elastic parameters:

$$\beta = 0{\cdot}5, 1 \quad \text{and} \quad \kappa = 1/30.$$

The values chosen for β are effectively lower and upper bounds for all unidirectional fibre reinforced composites, while the value chosen for κ is typical of CFRP. Table 1 below shows for various values of r_2/r_1, the corresponding values of $\sigma_{\theta,\max}$ expressed as a multiple of the nominal hoop stress $P/2(r_2 - r_1)$. These stress ratios can therefore be regarded as stress concentration factors.

TABLE 1

Values of $\sigma_{\theta,\max} \Big/ \left(\frac{P}{2(r_2 - r_1)}\right)$

	$r_2/r_1 = 1{\cdot}25$	1·5	2·0
$\beta = 0{\cdot}5, \kappa = 1/30$	9·69	8·51	10·83
$\beta = 1, \quad \kappa = 1/30$	10·34	9·51	12·07

Before discussing these results it is important to remember that they apply strictly to the load system depicted in Fig. 15b. Some general conclusions will now be drawn: The stress concentration factors are high but vary with r_2/r_1 by relatively small amounts; this is because as r_2/r_1 increases the component of the stress concentration factor due to the constant pressure term σ_θ^{**} increases, while that due to the bending component σ_θ^{*} decreases. Also, as β varies from 0·5 to 1 there is an increase in the stress concentration factor of about 10 per cent. Some such increase is to be expected because this change in the value of β, with κ constant, implies a reduction of about 50 per cent in the shear modulus $G_{r\theta}$.

Note that recent work suggests that the pressure distribution between the pin and ring is approximately constant. If this is so, it can be shown that the stress concentration factor increases monotonically with r_2/r_1, and at $r_2/r_1 = 2{\cdot}0$, $\kappa = 1/30$, for example, it is equal to about 4·0.

5. Conclusions

This Report considers the stress analysis of elastic plates with polar orthotropic properties. It is applicable to fibre reinforced composites in the form of an annulus or curved strip with circumferential fibres; in some circumstances it is also applicable to a multi-laminate composite. The simple loading conditions of pressure, moment and shear have been considered in detail and curves are presented which give the maximum stresses and other features for a wide range of composite geometries and elastic properties. As a general rule the stress concentration factors in the composite are higher than those in the corresponding isotropic case, though there are minor exceptions. In the derivation of the general form of the stress function certain differential operators are introduced which markedly simplify the subsequent analysis.

Acknowledgment

The author is much indebted to Miss Doreen Best for the computation.

LIST OF SYMBOLS

$E_r, E_\theta, G_{r\theta}$	Elastic moduli
I	$(r_2-r_1)^3/12$
J	Effective flexural rigidity
M	Moment per unit length
p	Pressure
P	Applied force per unit length
q	Index
r, θ	Polar coordinates
r_1, r_2	Inner and outer radii
S	Shear force per unit length
u, v	Radial and tangential displacements
$\alpha, \beta, \kappa, \omega, \eta$	Parameters defined by equations (8), (36), (51), (57)
Δ_r, Δ_θ	Differential operators defined by equation (35)
$\varepsilon_r, \varepsilon_\theta, \gamma_{r\theta}$	Direct and shear strains
Ψ, Φ	Stress functions defined by equations (5), (33)
μ	r_2/r_1
$\nu_{r\theta}, \nu_{\theta r}$	Poisson's ratios
ρ	r/r_1
$\sigma_r, \sigma_\theta, \tau_{r\theta}$	Direct and shear stresses
Ω	Rotation of section.

REFERENCES

No.	*Author(s)*	*Title, etc.*
1	S. G. Lekhnitskii	*Anisotropic Plates.* Translated from the second Russian edition by S. W. Tsai and T. Cheron. Gordon and Breach, 1968
2	J. E. Ashton and J. M. Whitney.....	*Theory of Laminated Plates.* Progress in Materials Science Series, Vol. IV. Technomic, 1970
3	W. S. Hemp	*Optimum Structures.* Clarendon Press, Oxford, 1973
4	P. Bartholomew and G. Z. Harris....	Optimum fibre-reinforced sheets for two alternative loadings. Int. J. mech. Sci., 15, pp. 1011–1025, 1973
5	E. H. Mansfield and D. R. Best.....	The concept of load diffusion length in fibre reinforced composites. A.R.C. C.P. 1338, 1975.
6	S. P. Timoshenko and J. N. Goodier .	*Theory of Elasticity.* 3rd edition, McGraw-Hill (1970)
7	J. H. Michell	Proc. Lond. math. Soc., Vol. 31, p. 100, 1899

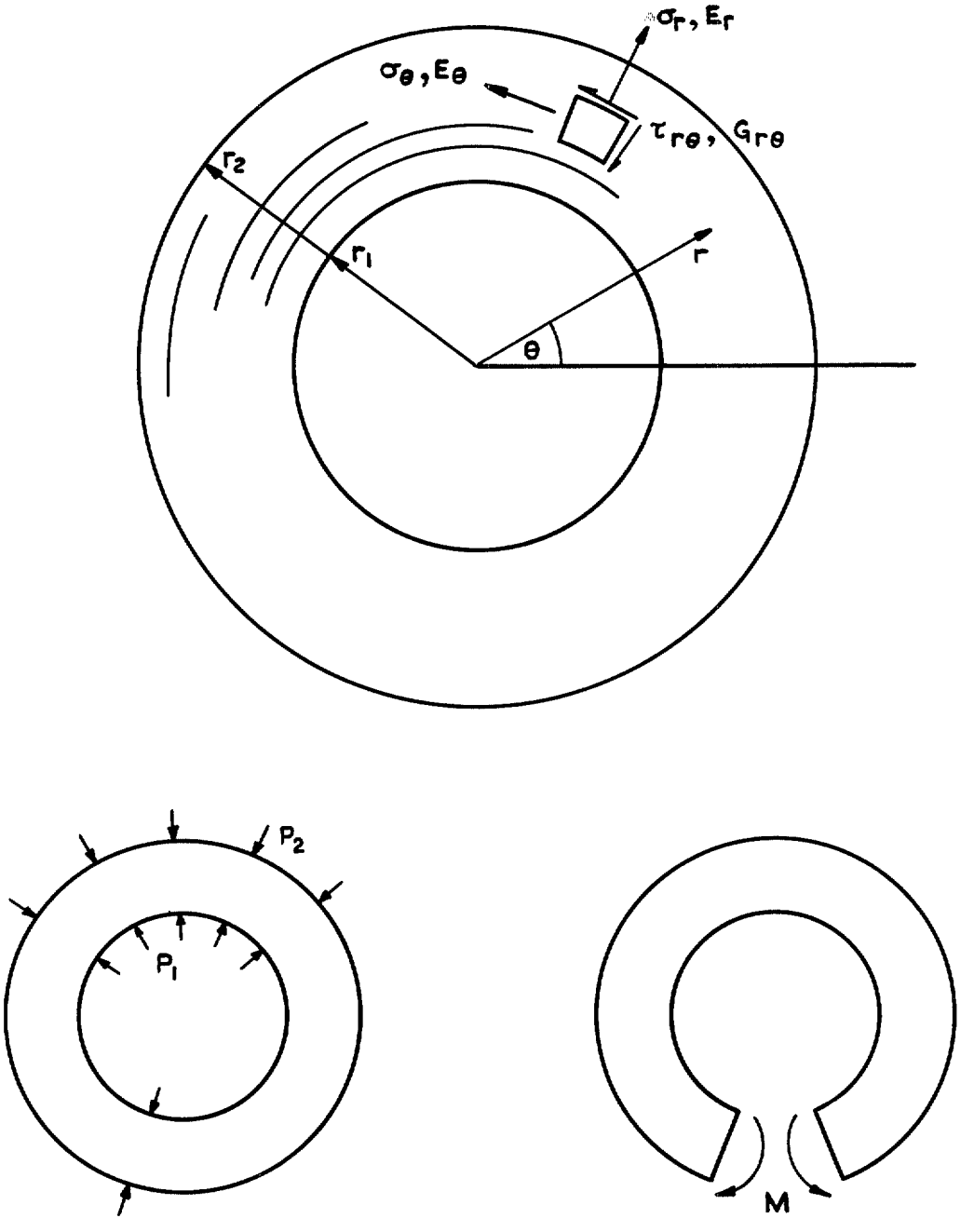

FIG. 1. Diagram showing notation.

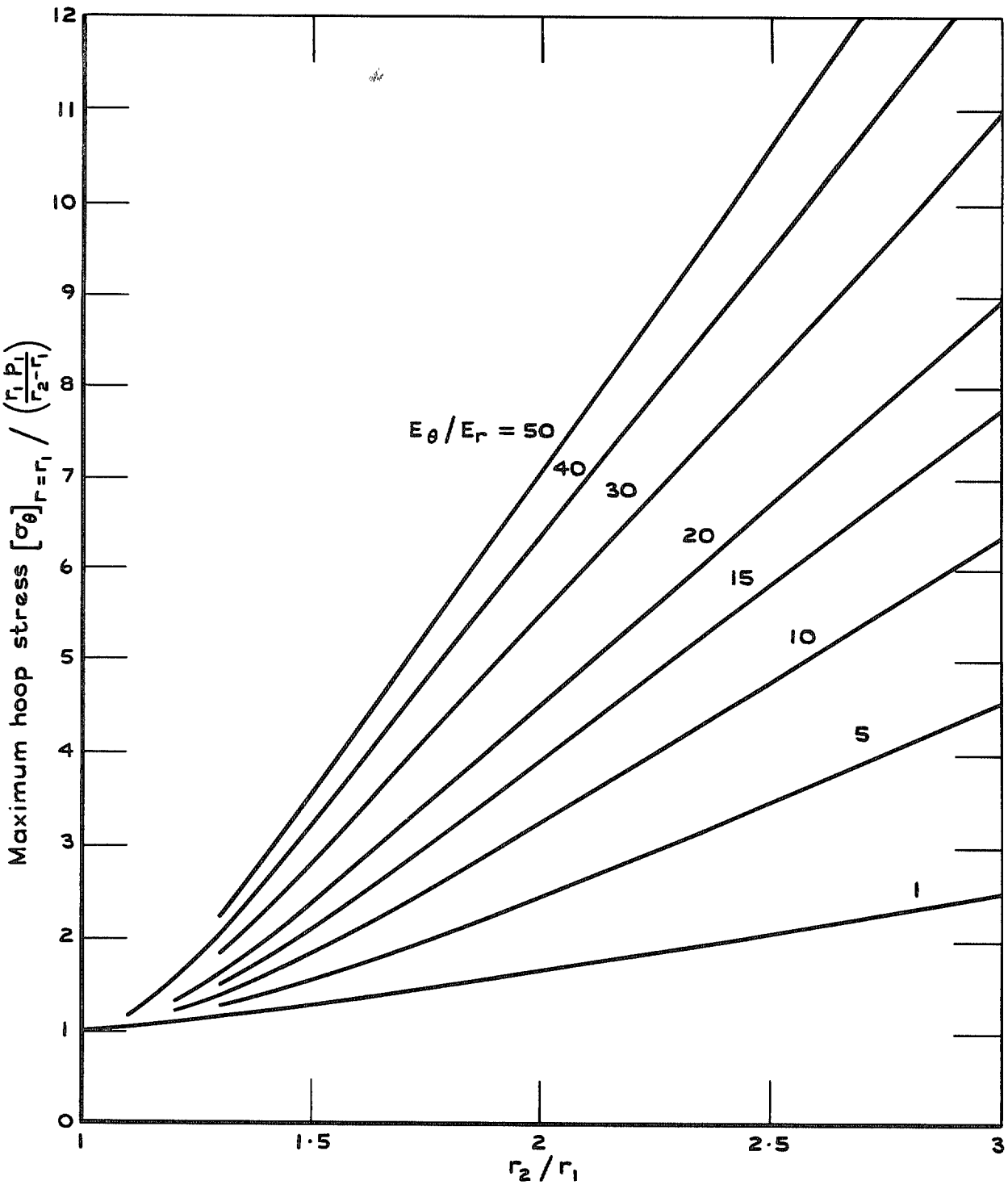

FIG. 2. Stress concentrations due to internal pressure p_1.

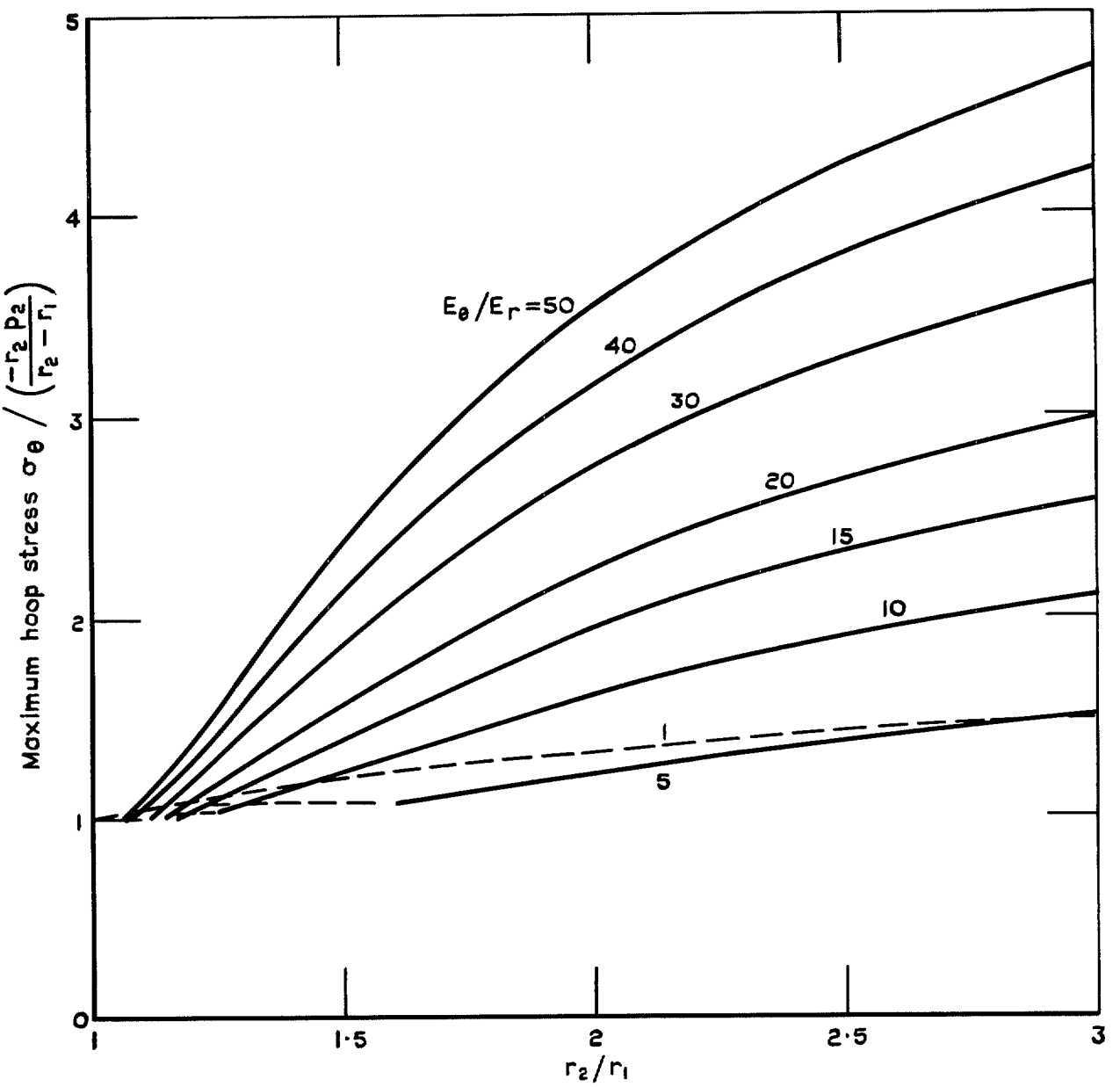

FIG. 3. Stress concentrations due to external pressure p_2.

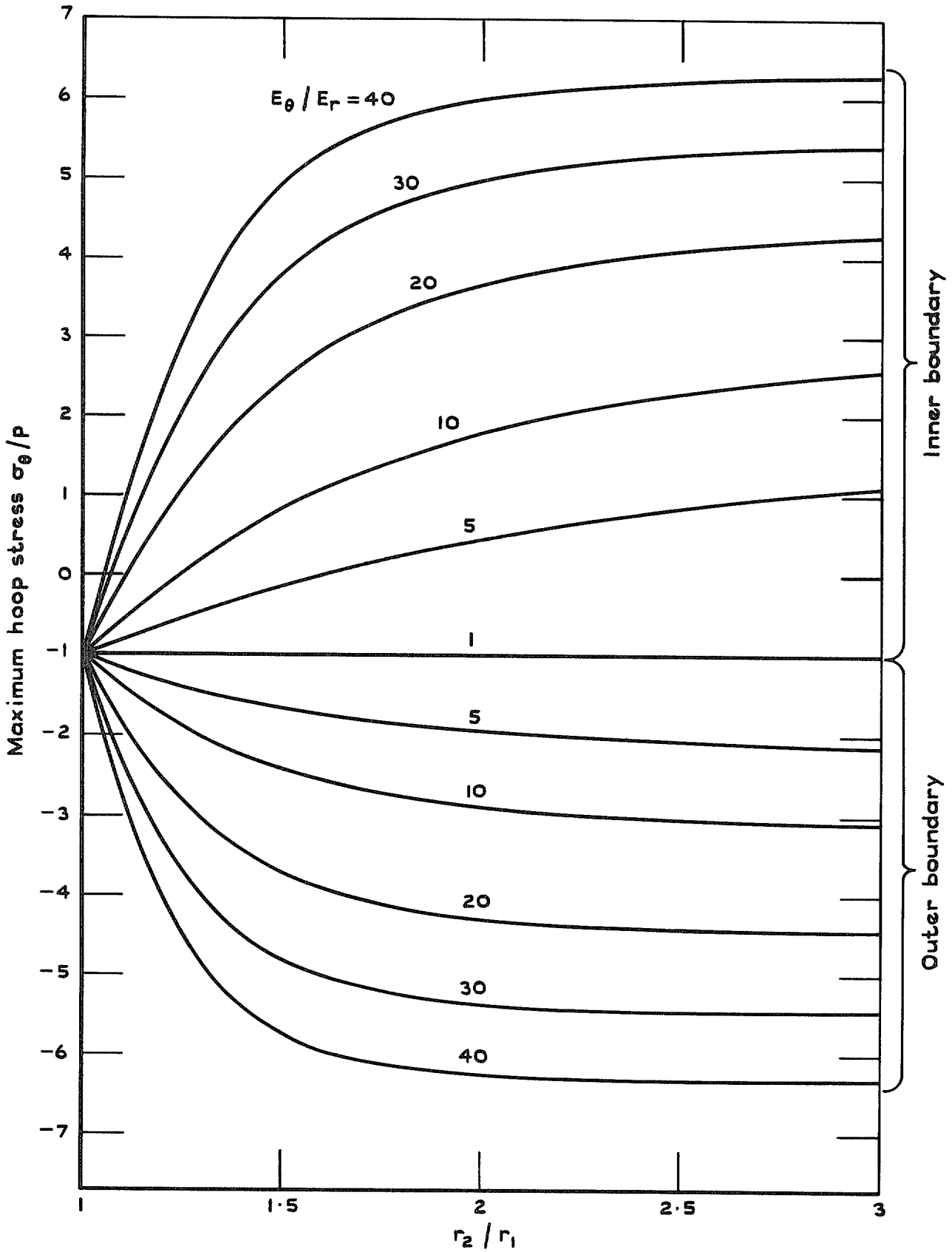

FIG. 4. Stress concentrations due to internal and external pressure p.

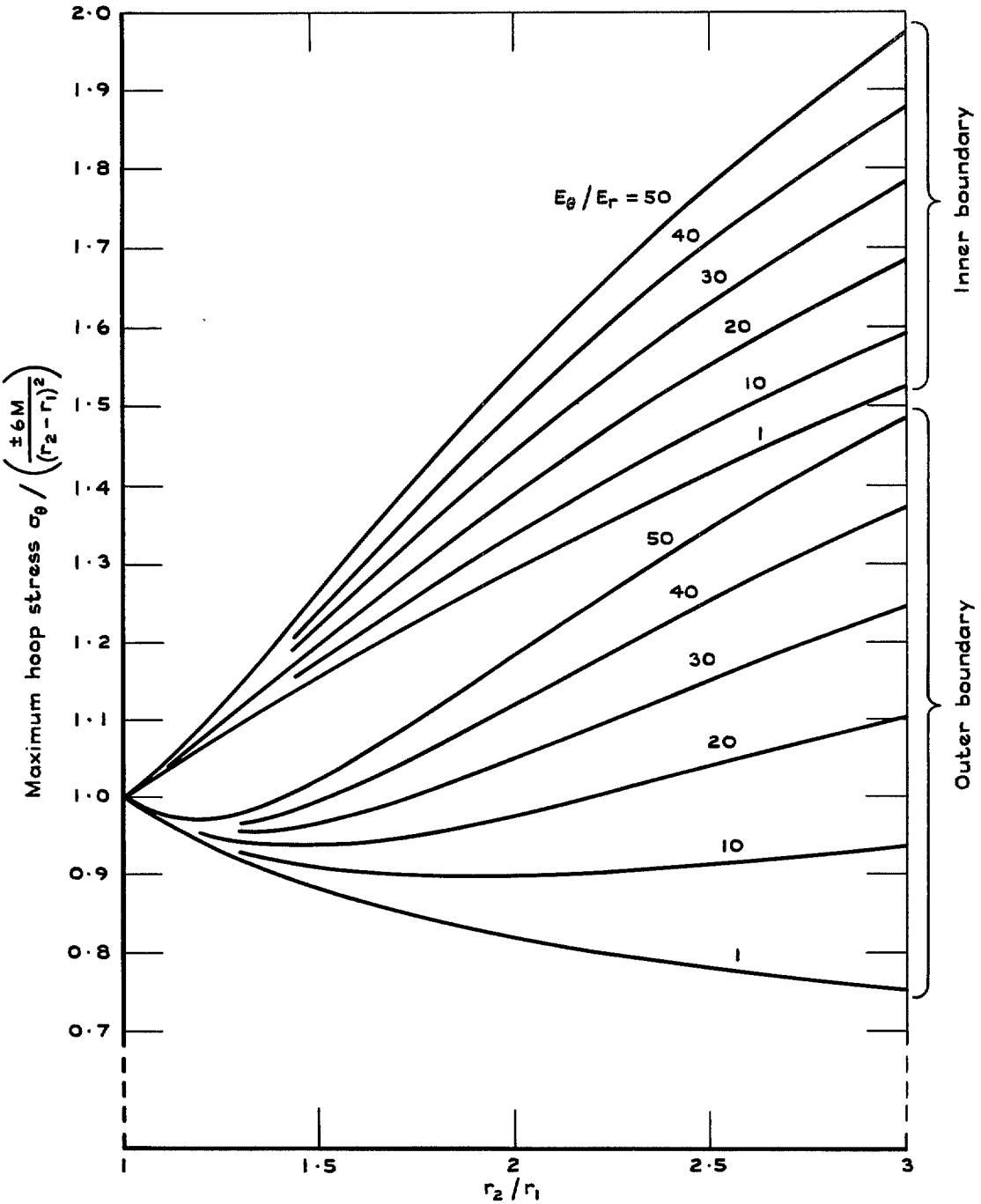

FIG. 5. Stress concentrations due to pure moment M.

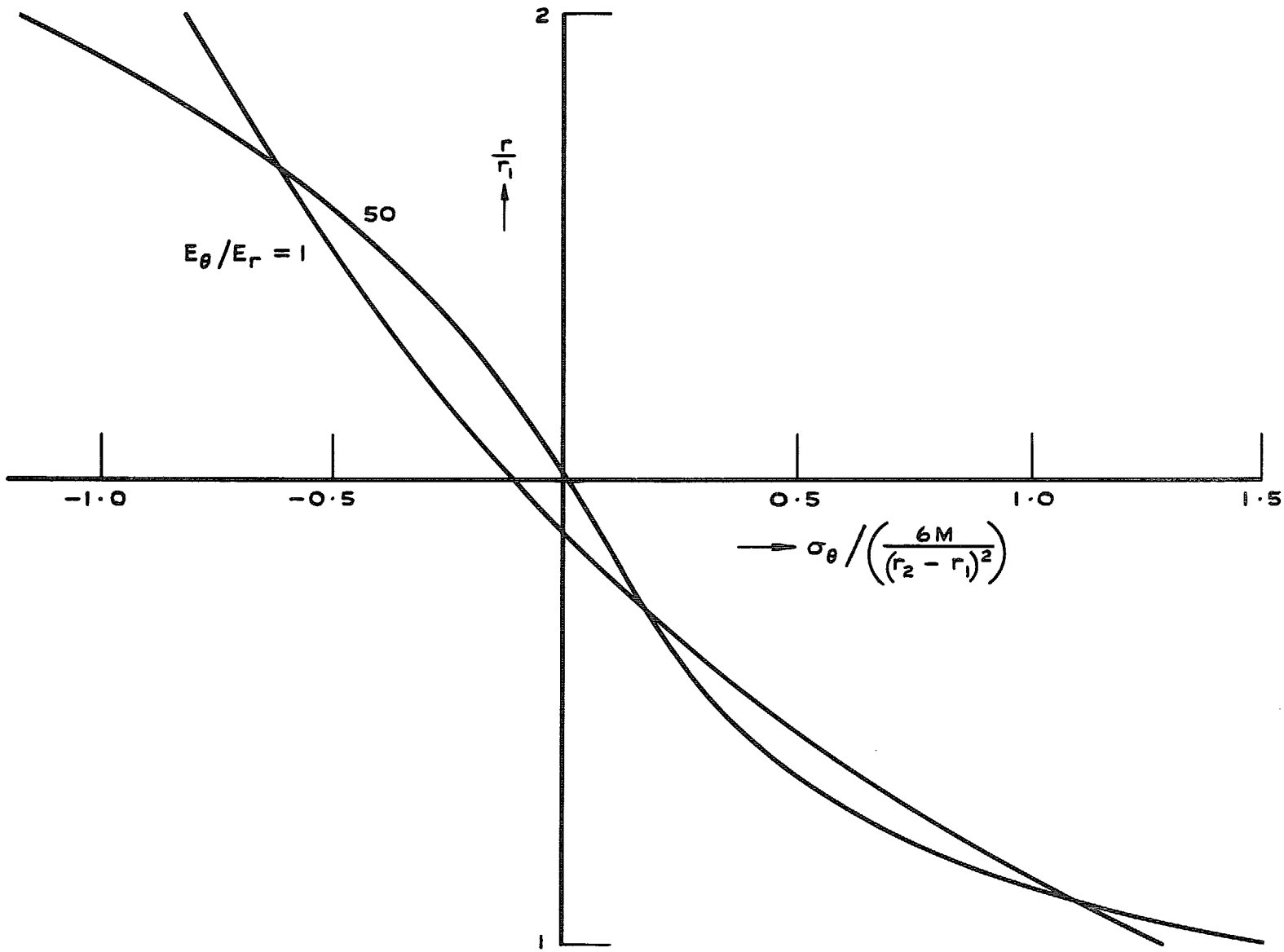

FIG. 6. Variation of hoop stress through thickness ($r_2/r_1 = 2$).

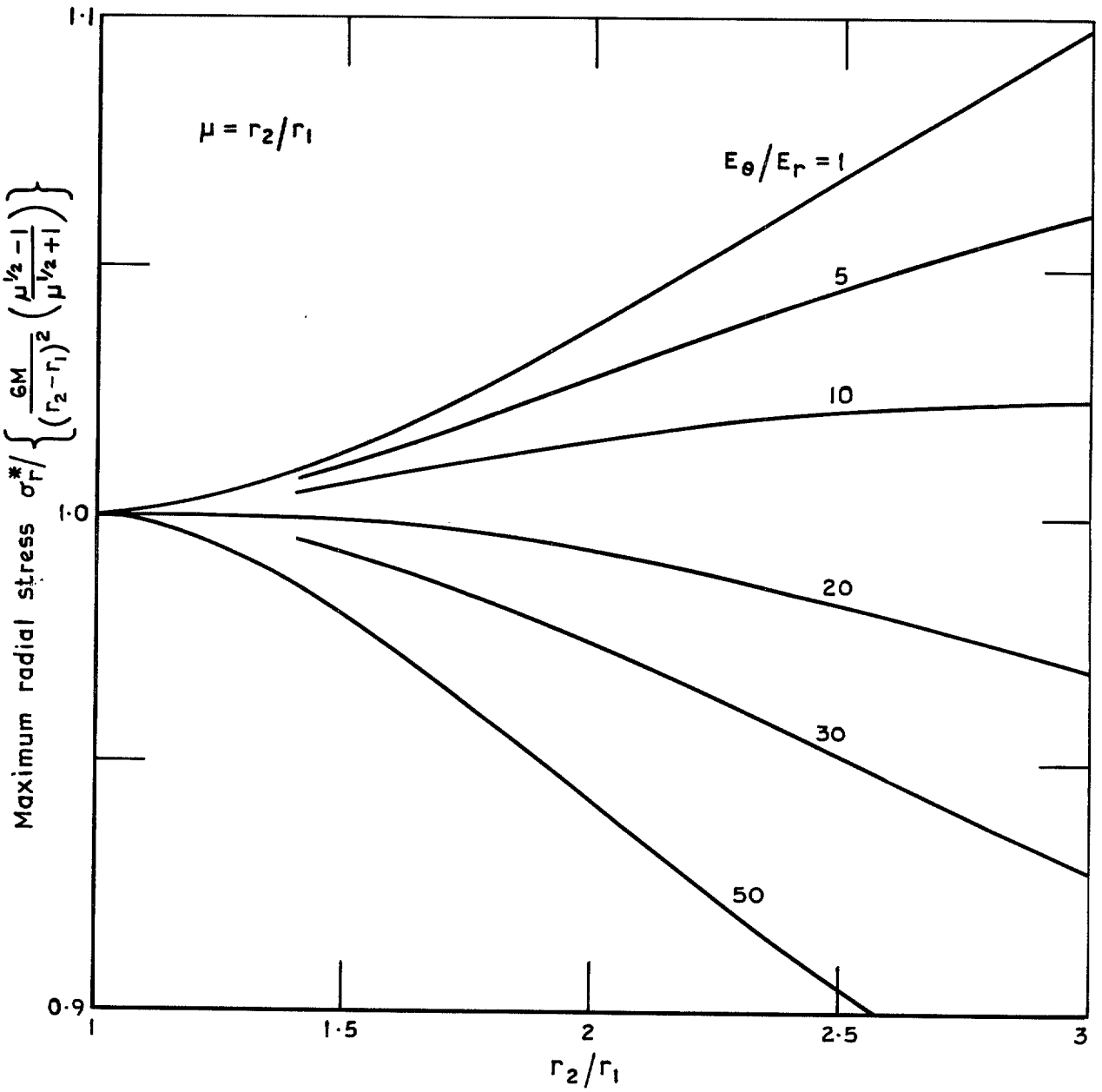

FIG. 7. Maximum radial stress due to pure moment M.

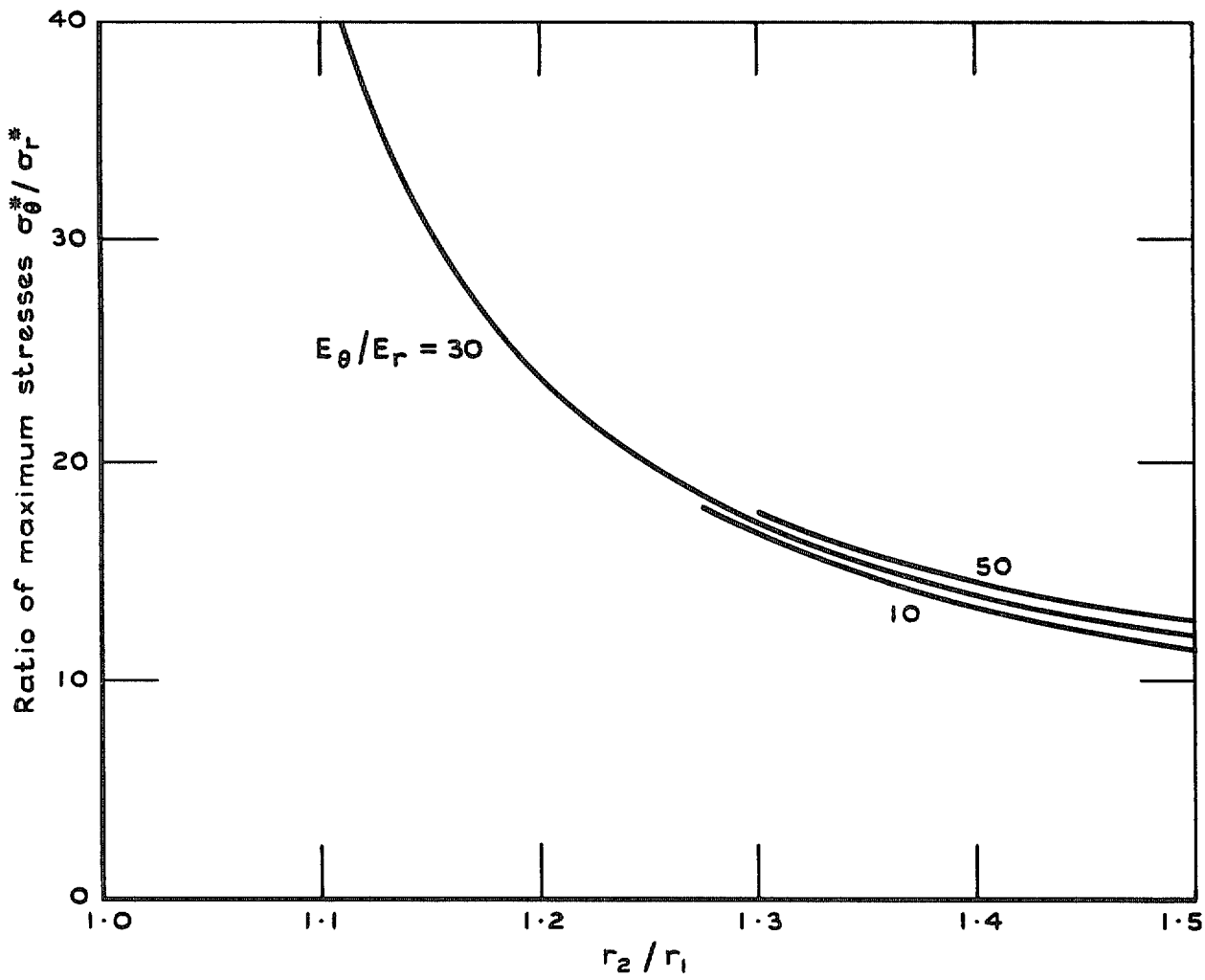

FIG. 8. Hoop to radial stress ratio under pure moment.

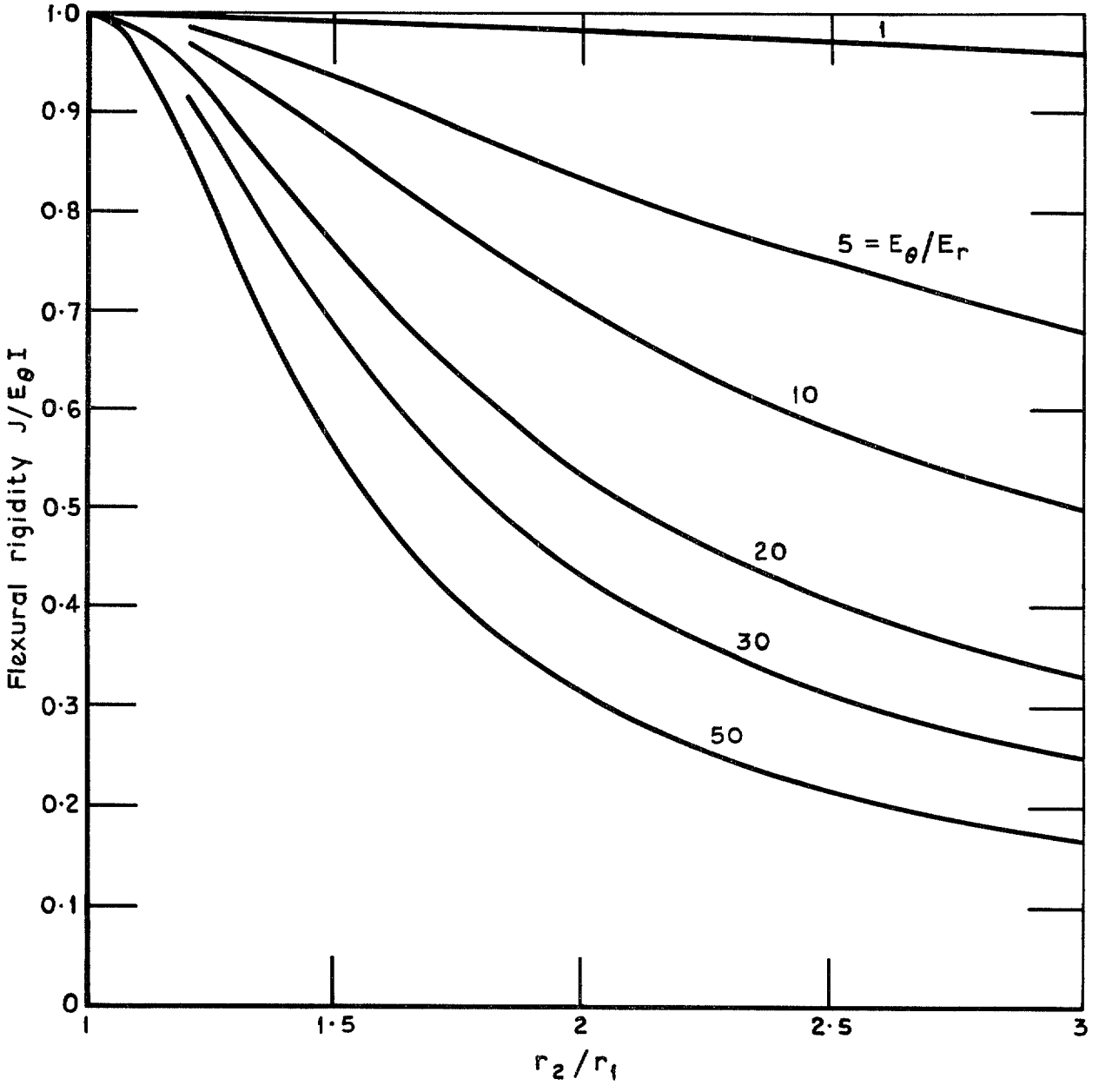

FIG. 9. Effective flexural rigidity of cut ring.

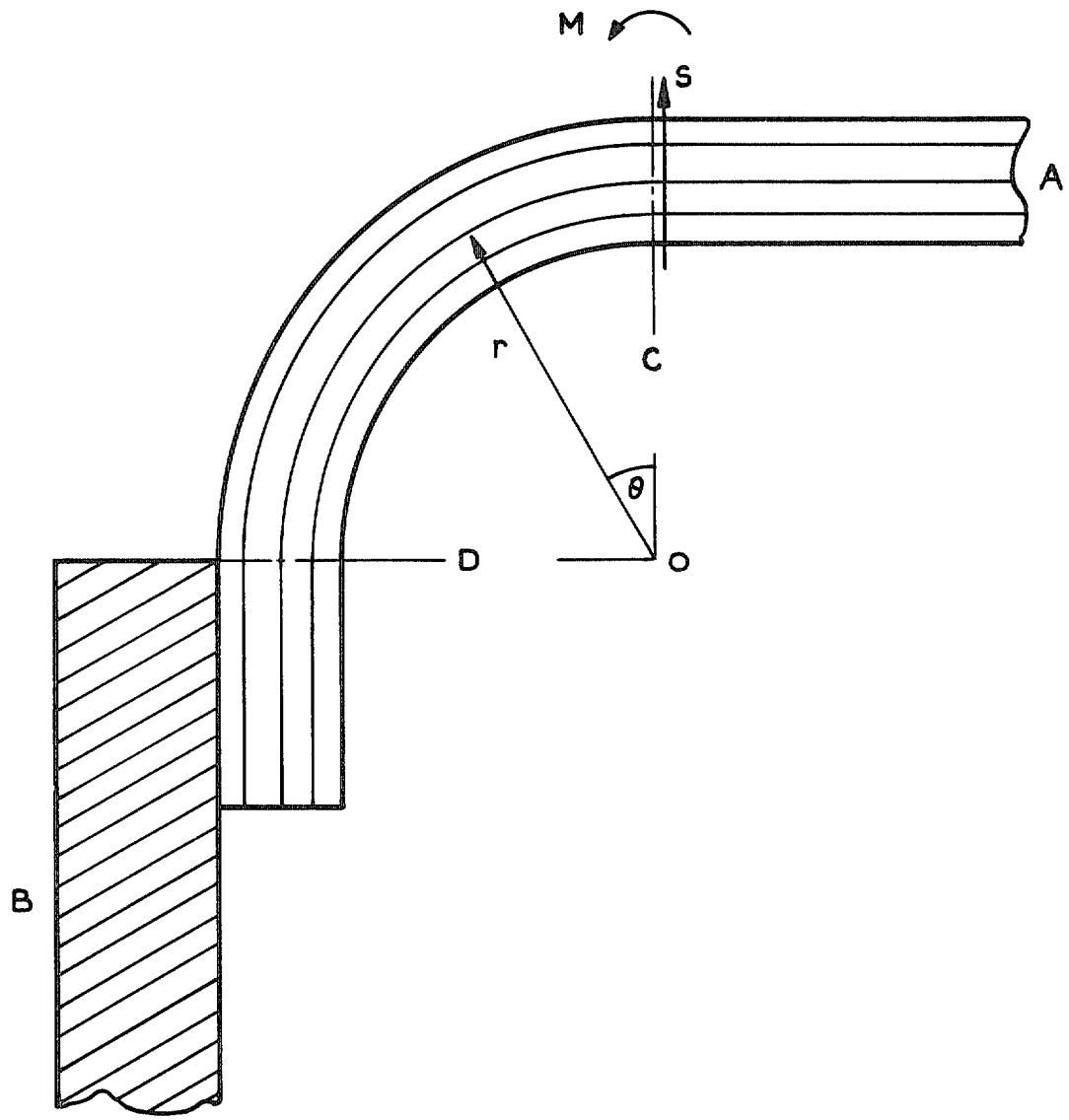

FIG. 10. Shear force applied to curved plate.

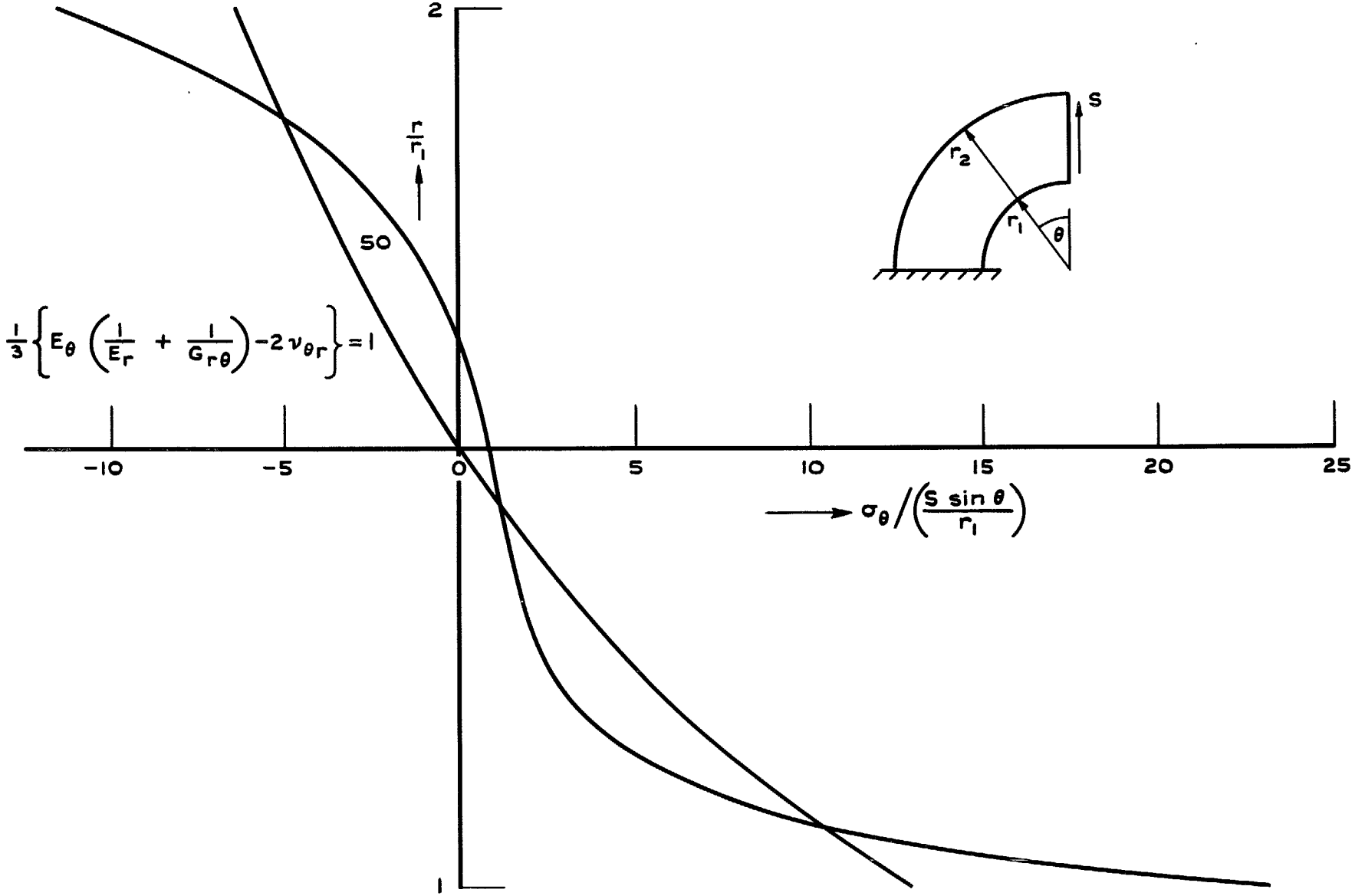

FIG. 11. Variation of hoop stress through thickness ($r_2/r_1 = 2$).

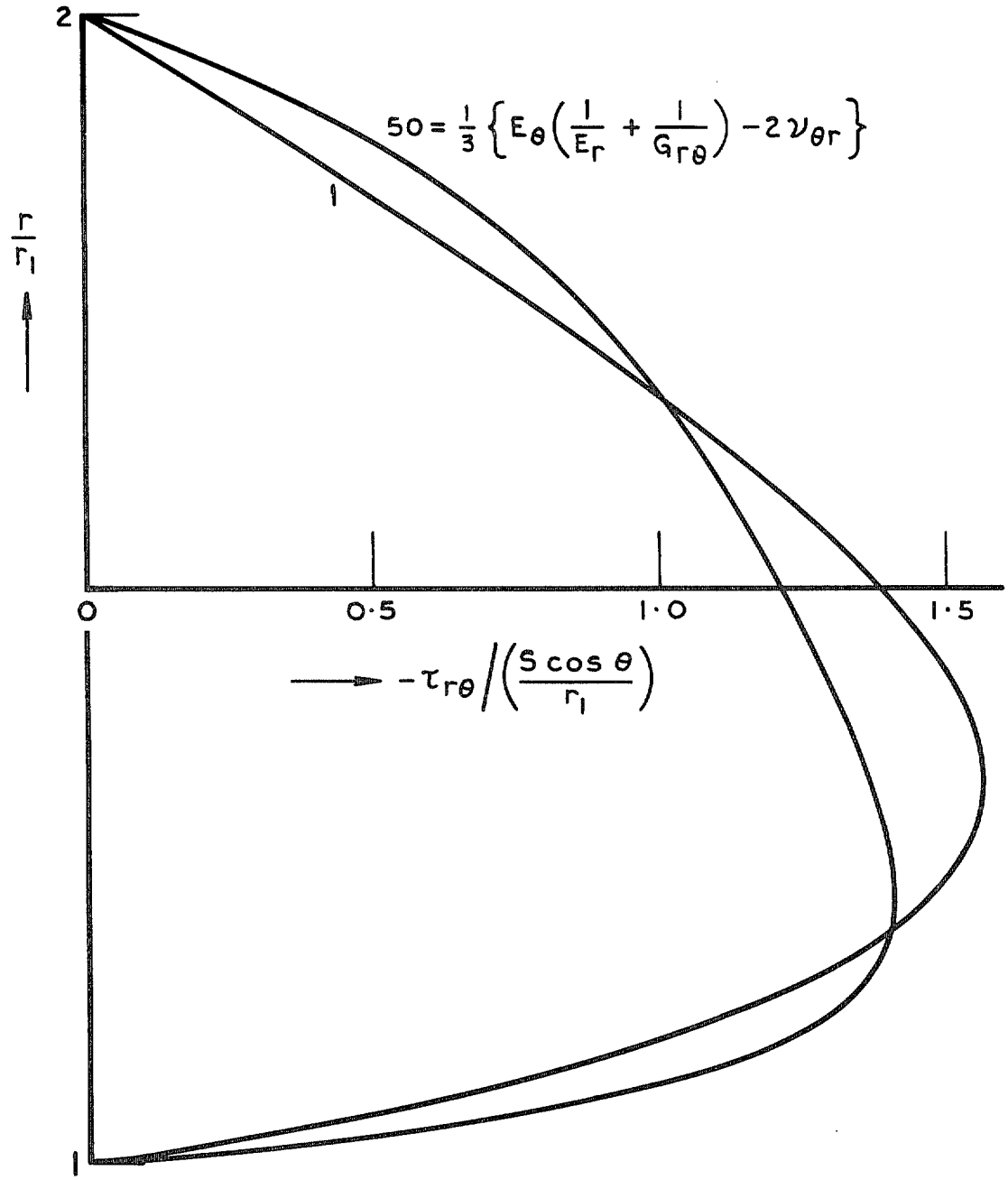

FIG. 12. Variation of shear stress through thickness ($r_2/r_1 = 2$).

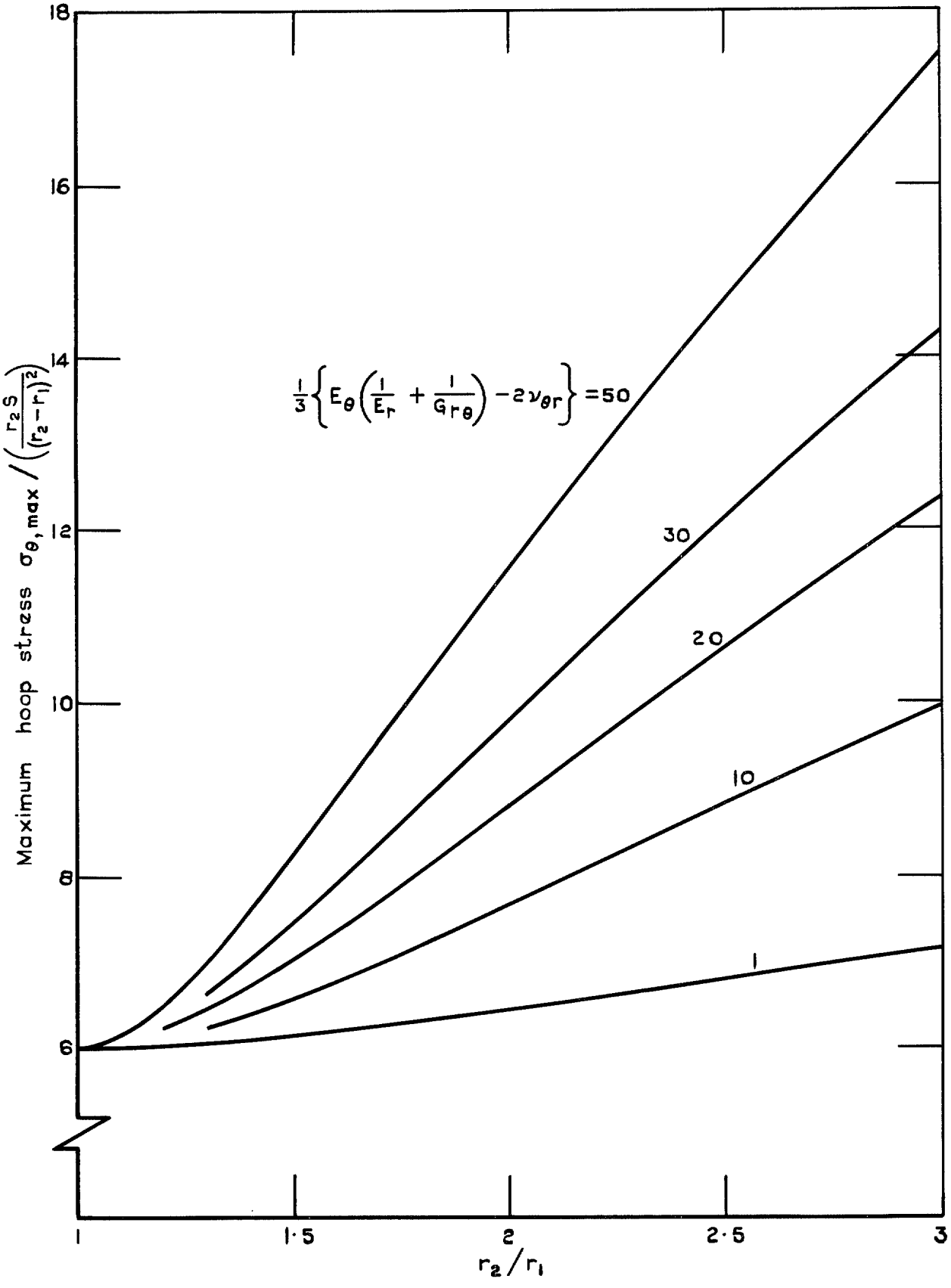

FIG. 13. Maximum hoop stress due to shear force.

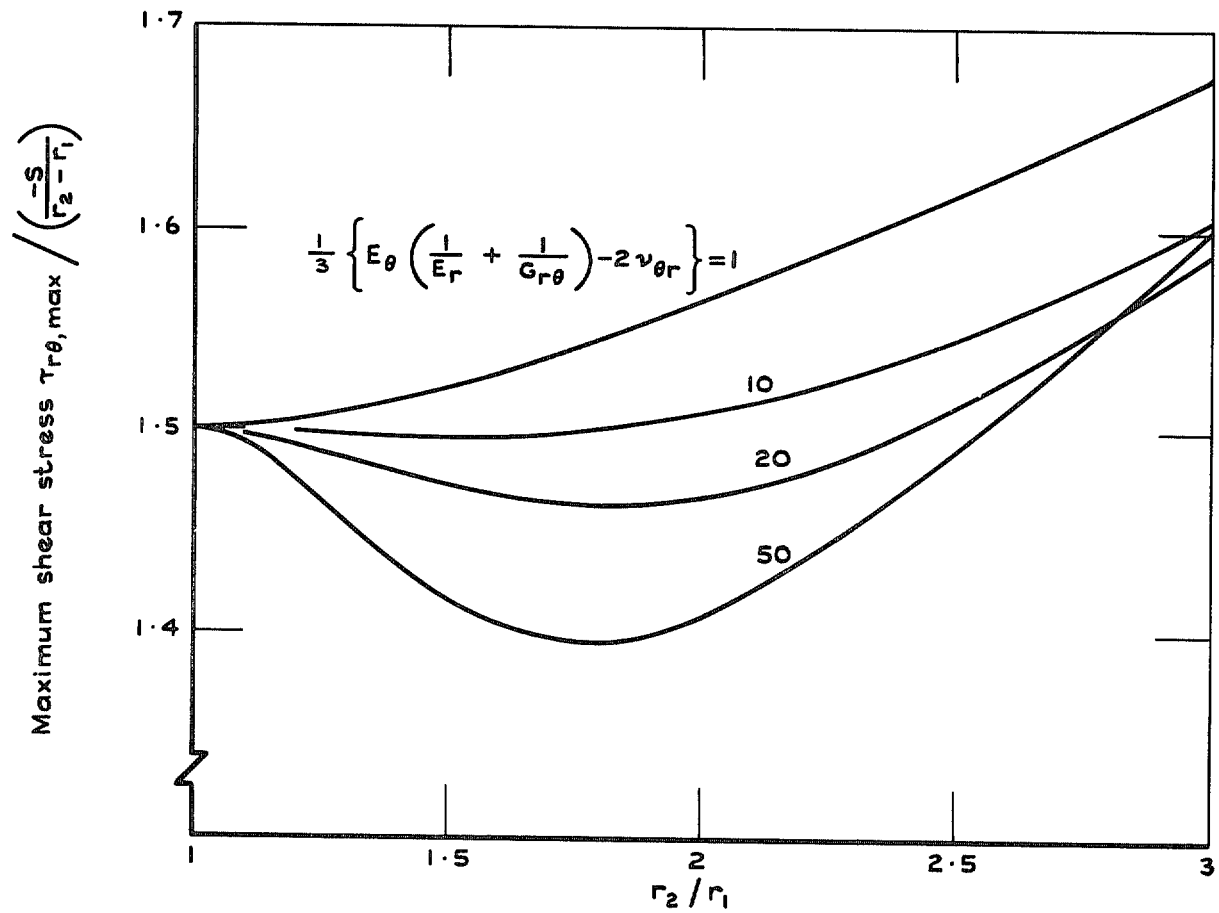

FIG. 14. Maximum shear stress in curved beam.

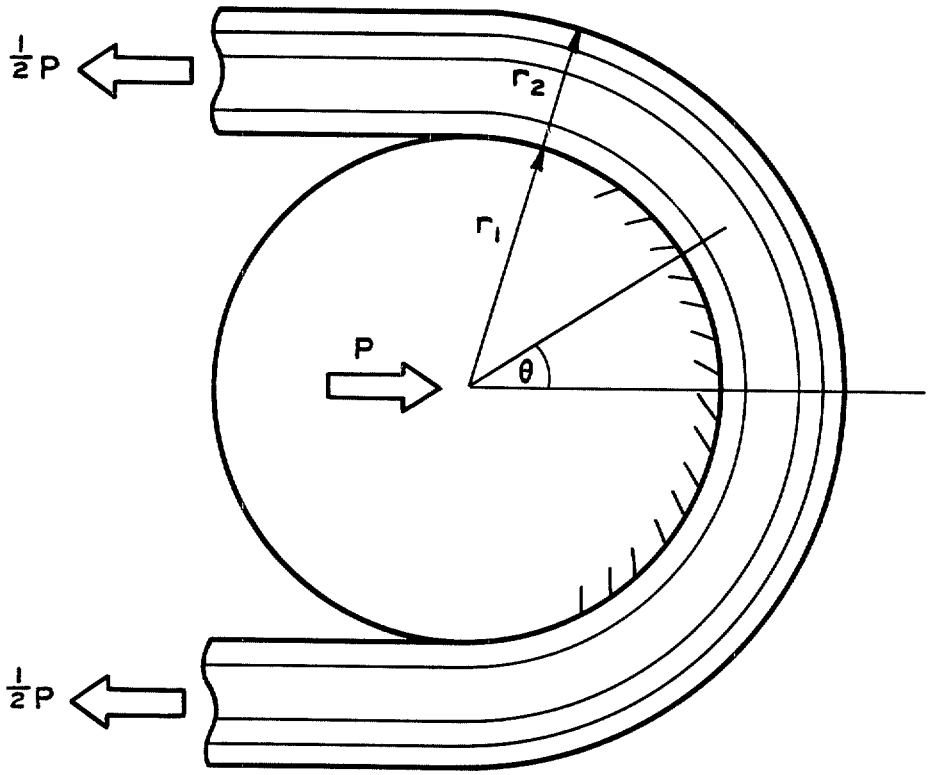

a

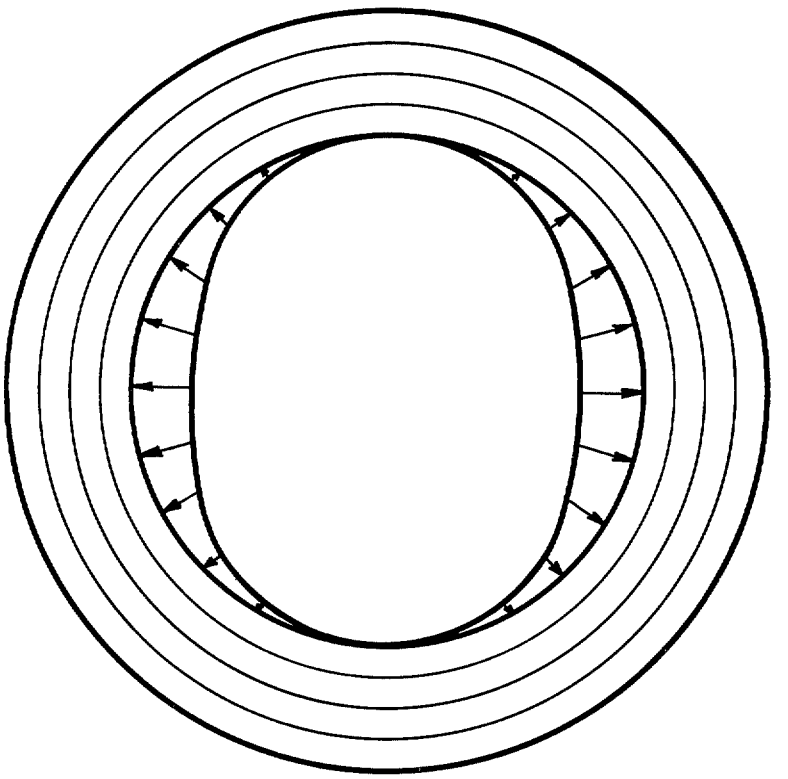

b

FIG. 15a & b. Load transfer via semi-circular ring.

Printed in England for Her Majesty's Stationery Office by J. W. Arrowsmith Ltd., Bristol BS3 2NT
Dd. 290278 K.5. 2/77.

HER MAJESTY'S STATIONERY OFFICE

Government Bookshops

49 High Holborn, London WC1V 6HB
13a Castle Street, Edinburgh EH2 3AR
41 The Hayes, Cardiff CF1 1JW
Brazennose Street, Manchester M60 8AS
Southey House, Wine Street, Bristol BS1 2BQ
258 Broad Street, Birmingham B1 2HE
80 Chichester Street, Belfast BT1 4JY

Government Publications are also available through booksellers

ISBN 0 11 470967 X